Journal of Statistical Physics, Vol. 94, Nos. 3/4, 1999

Fokker–Planck Equation, Molecular Friction, and Molecular Dynamics for Brownian Particle Transport near External Solid Surfaces

Michael H. Peters[1]

Received April 20, 1998; final June 12, 1998

The Fokker–Planck (FP) equation describing the dynamics of a single Brownian particle near a fixed external surface is derived using the multiple-time-scales perturbation method, previously used by Cukier and Deutch and Nienhuis in the absence of any external surfaces, and Piasecki *et al.* for two Brownian spheres in a hard fluid. The FP equation includes an explicit expression for the (time-independent) particle friction tensor in terms of the force autocorrelation function and equilibrium average force on the particle by the surrounding fluid and in the presence of a fixed external surface, such as an adsorbate. The scaling and perturbation analysis given here also shows that the force autocorrelation function must decay rapidly on the zeroth-order time scale τ_0, which physically requires $N_{\mathbf{Kn}} \ll 1$, where $N_{\mathbf{Kn}}$ is the Knudsen number (ratio of the length scale for fluid intermolecular interactions to the Brownian particle length scale). This restricts the theory given here to liquid systems where $N_{\mathbf{Kn}} \ll 1$. For a specified particle configuration with respect to the external surface, equilibrium canonical molecular dynamics (MD) calculations are conducted, as shown here, in order to obtain numerical values of the friction tensor from the force autocorrelation expression. Molecular dynamics computations of the friction tensor for a single spherical particle in the absence of a fixed external surface are shown to recover Stokes' law for various types of fluid molecule–particle interaction potentials. Analytical studies of the static force correlation function also demonstrate the remarkable principle of force-time parity whereby the particle friction coefficient is nearly independent of the fluid molecule–particle interaction potential. Molecular dynamics computations of the friction tensor for a single spherical particle near a fixed external spherical surface (adsorbate)

[1] Department of Chemical Engineering, College of Engineering, Florida State University and Florida A & M University, Tallahassee, Florida 32310; e-mail: peters@eng.fsu.edu.

0022-4715/99/0200-0557$16.00/0 © 1999 Plenum Publishing Corporation

demonstrate a breakdown in continuum hydrodynamic results at close particle–surface separation distances on the order of several molecular diameters.

KEY WORDS: Brownian particle; Fokker–Planck equation; adsorption; molecular friction; force autocorrelation function; molecular dynamics.

1. INTRODUCTION

The behavior of small, Brownian particles near surfaces represents an important practical problem for a variety of processes involving adsorption and separation of small macromolecules, such as proteins. Despite this importance, no general scheme for including all aspects of the problem, such as complex physical shapes of particles and surfaces and the differences in the "chemistry" or specific molecular interactions, currently exists. Most studies are based on continuum approximations to the effective hydrodynamics with idealized shapes of surfaces and particles, such as spheres, cylinders, etc. The fact that the "chemistry" of the interactions can be important is evident from recent studies of protein dynamics with observed violations in the Stokes–Einstein relation.[1, 2] In these studies, deviations in the intrinsic transport properties of the solvent due to the presence of particles were observed. Clearly, it would be desirable to have a systematic method of determining the dynamics of small particles near surfaces that is "built" from the molecular scale and that would intrinsically include all surface-solvent-solute interactions. Unfortunately, it is not computationally conceivable to utilize purely molecular dynamics methods, with time steps on the order of 10^{-14} seconds, since the time scales of interest in adsorption and separation of small particles or macromolecules are on the order of seconds.

In a previous study,[3] a molecular dynamics method was used to study the behavior of the many-bodied friction tensor for particles immersed in a rarefied, "free-molecule" gas. In that study, it was noted that the molecular dynamics method could be used to study the long-time behavior of Brownian particles by a two-step procedure. In the first step, for a given particle configuration, the many-body friction tensor is determined from molecular dynamics (MD) through the analysis of the force autocorrelation function. In this step, the particle coordinates are kept fixed according to the fluctuation-dissipation type relation that gives the (time-independent) friction tensor in terms of the force autocorrelation function. In the second step, the Fokker–Planck (FP) equation for the Brownian particle is solved for discrete times assuming that the friction tensor remains constant over the time step [Brownian Dynamics (BD) method]. The particles are advanced to new positions according to the integrated FP equation and the

entire process, MD followed by BD is repeated. Thus, MD is only performed at the beginning of each BD time step. As will be shown here, for the method to be successful, the force autocorrelation function must decay rapidly (on the order of picoseconds).

In this study, beginning with the Liouville equation, we derive the generalized Fokker–Planck (FP) equation for a Brownian particle near a wall using the method of multiple time scales. It is shown that new terms arise in the FP equation due to the presence of a wall. The relation between the friction tensor for the particle and the force autocorrelation function is also obtained. This relationship is shown to reduce to well-known results in the absence of a wall. In Section 3, specific molecular dynamics simulations are given for the force autocorrelation function. Comparisons to analytical results for idealized geometries are also given. We note that the problem of a single Brownian particle near a fixed surface is fundamentally similar to the problem of two, interacting Brownian particles where one particle is held fixed.

2. GENERALIZED FOKKER–PLANCK EQUATION FOR BROWNIAN PARTICLE TRANSPORT NEAR A WALL

We begin with Liouville equation for the entire system, N fluid molecules plus particle,

$$\frac{\partial f}{\partial t} = -(L_f + L_p)\, f \tag{1}$$

where $f(\mathbf{r}^N, \mathbf{p}^N, \mathbf{R}, \mathbf{P}, \mathbf{t})$ is the probability of finding N fluid molecules at $(\mathbf{r}^N, \mathbf{p}^N)$ and a particle at $(\mathbf{R}, \mathbf{P})$, both at time t. L_f and L_p are the Liouville operators for the fluid molecules and particle, respectively,

$$L_f = \sum_{i=1}^{N} \left\{ \frac{\mathbf{p}_i}{m} \cdot \frac{\partial}{\partial \mathbf{r}_i} - \frac{\partial}{\partial \mathbf{r}_i} \left[u_{fp}(\mathbf{r}_i - \mathbf{R}) + u_{fw}(\mathbf{r}_i - \mathbf{R}_w) + \sum_{j=1,\, j<i}^{N} u_{ff}(\mathbf{r}_i - \mathbf{r}_j) \right] \cdot \frac{\partial}{\partial \mathbf{p}_i} \right\} \tag{2}$$

$$L_p = \frac{\mathbf{P}}{M} \cdot \frac{\partial}{\partial \mathbf{R}} - \frac{\partial}{\partial \mathbf{R}} \left[\sum_{i=1}^{N} u_{fp}(\mathbf{r}_i - \mathbf{R}) + u_{pw}(\mathbf{R} - \mathbf{R}_w) \right] \cdot \frac{\partial}{\partial \mathbf{P}} \tag{3}$$

where u_{fp}, u_{fw}, u_{ff}, and u_{pw} are the interaction potentials between molecule-particle, molecule-wall, molecule-molecule, and particle-wall; also, m is the mass of a single molecule and M is the mass of the particle. Note that to succinctly illustrate wall effects, we are neglecting the rotational degrees of

freedom for the particle; rotational motions will be considered in a subsequent paper. Next, the following dimensionless "scaled" variables are introduced

$$f^* = \frac{f}{f_0} \tag{4}$$

$$\mathbf{p}_i^* = \frac{\mathbf{p}_i}{(mkT)^{1/2}} \tag{5}$$

$$\mathbf{r}_i^* = \frac{\mathbf{r}_i}{r_0} \tag{6}$$

$$\mathbf{P}^* = \frac{\mathbf{P}}{(M\,kT)^{1/2}} \tag{7}$$

$$\mathbf{R}^* = \frac{\mathbf{R}}{R_0} \tag{8}$$

$$u_{lk}^* = \frac{u_{lk}}{kT}; \qquad lk = fp,\ fw,\ ff,\ pw \tag{9}$$

and

$$t^* = \frac{t}{t_0} = \frac{t(kT/m)^{1/2}}{R_0} \tag{10}$$

Note that $t_0[= R_0/(kT/m)^{1/2}]$ is a characteristic fluid molecule-Brownian particle interaction time.

Substituting the dimensionless variables into Eq. (1) gives

$$\frac{\partial f^*}{\partial t^*} = -(N_{\mathrm{Kn}}^{-1} L_f^* + \gamma L_p^*)\, f^* \tag{11}$$

where $N_{\mathrm{Kn}}^{-1} \equiv R_0/r_0$ is a type of Knudsen number, R_0 is a characteristic Brownian particle length scale, r_0 is a characteristic length scale for fluid intermolecular interaction forces,

$$L_f^* = \sum_{i=1}^{N} \left\{ \mathbf{p}_i^* \cdot \frac{\partial}{\partial \mathbf{r}_i^*} - \frac{\partial}{\partial \mathbf{r}_i^*} [\, u_{fp}^* + u_{fw}^* + u_{ff}^*] \cdot \frac{\partial}{\partial \mathbf{p}_i^*} \right\} \tag{12}$$

$$L_p^* = \mathbf{P}^* \cdot \frac{\partial}{\partial \mathbf{R}^*} - \frac{\partial}{\partial \mathbf{R}^*} \left[\left(\sum_{i=1}^{N} u_{fp}^* \right) + u_{pw}^* \right] \cdot \frac{\partial}{\partial \mathbf{P}^*} \tag{13}$$

and $\gamma = (m/M)^{1/2}$ is the square root of the mass of a molecule over that of the particle. The so-called Brownian particle behavior is obtained by considering the asymptotic behavior of Eq. (11) under the conditions $\gamma \ll 1$. For ease of notation, we will henceforth drop the asterisk notation; all quantities will be implicitly dimensionless unless otherwise indicated.

The Brownian particle probability distribution function is defined according to

$$\Psi(\mathbf{R}, \mathbf{P}, t) = \int_{\text{all } \mathbf{r}^N,\, \mathbf{p}^N} f(\mathbf{r}^N, \mathbf{p}^N, \mathbf{R}, \mathbf{P}, t)\, d\mathbf{r}^N\, d\mathbf{p}^N \tag{14}$$

In a general fashion, we can integrate Eq. (11) over the phase-space of the fluid molecules to obtain

$$\frac{\partial \Psi}{\partial t} = \gamma \left[-\mathbf{P} \cdot \frac{\partial \Psi}{\partial \mathbf{R}} + \frac{\partial u_{pw}}{\partial \mathbf{R}} \cdot \frac{\partial \Psi}{\partial \mathbf{P}} + \mathscr{L} f \right] \tag{15}$$

where

$$\mathscr{L} f \equiv \int \left\{ \frac{\partial}{\partial \mathbf{R}} \left[\sum_{i=1}^{N} u_{fp}(\mathbf{r}_i - \mathbf{R}) \right] \cdot \frac{\partial f}{\partial \mathbf{P}} \right\} d\mathbf{r}^N\, d\mathbf{p}^N \tag{16}$$

Equation (15) is a formal albeit unresolved result; to proceed further, we must resolve Eq. (16). Here we follow the multiple time scales method previously used by Cukier and Deutch[4] and Nienhuis[5] in the absence of wall effects. It will be shown here that wall effects alter the particle dynamics in many different ways. The results given are also consistent with those obtained by Piasecki *et al.*[6] for two Brownian particles in a hard fluid.

For $\gamma \ll 1$, we consider the following multiple time scale expansions to the probability distribution functions

$$\begin{aligned} f &= f(\mathbf{r}^N, \mathbf{p}^N, \mathbf{R}, \mathbf{P}, \tau_0, \tau_1, \tau_2, \ldots) \\ &= f^{(0)}(\mathbf{r}^N, \mathbf{p}^N, \mathbf{R}, \mathbf{P}, \tau_0, \tau_1, \tau_2, \ldots) + \gamma f^{(1)} + \gamma^2 f^{(2)} + \cdots \end{aligned} \tag{17}$$

and

$$\begin{aligned} \Psi &= \Psi(\mathbf{R}, \mathbf{P}, \tau_0, \tau_1, \tau_2, \ldots) \\ &= \Psi^{(0)}(\mathbf{R}, \mathbf{P}, \tau_0, \tau_1, \tau_2, \ldots) + \gamma \Psi^{(1)} + \gamma^2 \Psi^{(2)} + \cdots \end{aligned} \tag{18}$$

where $\tau_n = \gamma^n t$ are the various time scales: τ_0 reflects the dynamics for small times, τ_1 for somewhat larger times, etc. In the multiple time scales method,

the introduction of new independent time variables allows us to introduce "new conditions" on the solution behavior that need not have any physical basis.[7] Substituting Eq. (17) and Eq. (18) into Eq (11) and Eq. (15), with $\partial/\partial t = \partial/\partial\tau_0 + \gamma(\partial/\partial\tau_1) + \gamma^2(\partial/\partial\tau_2) + \cdots$, gives the following set of problems

$$\frac{\partial f^{(0)}}{\partial \tau_0} = -N_{\mathrm{Kn}}^{-1} L_f f^{(0)} \tag{19}$$

$$\frac{\partial f^{(1)}}{\partial \tau_0} + \frac{\partial f^{(0)}}{\partial \tau_1} = -[N_{\mathrm{Kn}}^{-1} L_f f^{(1)} - L_p f^{(0)}] \tag{20}$$

$$\frac{\partial f^{(2)}}{\partial \tau_0} + \frac{\partial f^{(1)}}{\partial \tau_1} + \frac{\partial f^{(0)}}{\partial \tau_2} = -[N_{\mathrm{Kn}}^{-1} L_f f^{(2)} - L_p f^{(1)}] \tag{21}$$

etc. and

$$\frac{\partial \Psi^{(0)}}{\partial \tau_0} = 0 \tag{22}$$

$$\frac{\partial \Psi^{(1)}}{\partial \tau_0} + \frac{\partial \Psi^{(0)}}{\partial \tau_1} = \left[-\mathbf{P} \cdot \frac{\partial \Psi^{(0)}}{\partial \mathbf{R}} + \frac{\partial u_{pw}}{\partial \mathbf{R}} \cdot \frac{\partial \Psi^{(0)}}{\partial \mathbf{P}} + \mathscr{L} f^{(0)} \right] \tag{23}$$

$$\frac{\partial \Psi^{(2)}}{\partial \tau_0} + \frac{\partial \Psi^{(1)}}{\partial \tau_1} + \frac{\partial \Psi^{(0)}}{\partial \tau_2} = \left[-\mathbf{P} \cdot \frac{\partial \Psi^{(1)}}{\partial \mathbf{R}} + \frac{\partial u_{pw}}{\partial \mathbf{R}} \cdot \frac{\partial \Psi^{(1)}}{\partial \mathbf{P}} + \mathscr{L} f^{(1)} \right] \tag{24}$$

etc.

As given previously by Cukier and Deutch,[4] the solutions to Eqs. (22) and (19) are, respectively

$$\Psi^{(0)} = \Psi^{(0)}(\mathbf{Q}, \tau_1, \tau_2, \ldots), \qquad \text{or} \qquad \Psi^{(0)} \neq \Psi^{(0)}(\tau_0) \tag{25}$$

and

$$f^{(0)}(\mathbf{q}, \mathbf{Q}, \tau_0, \tau_1, \ldots) = e^{-N_{\mathrm{Kn}}^{-1} L_f \tau_0} f^{(0)}(\mathbf{q}, \mathbf{Q}, 0, \tau_1, \ldots) \tag{26}$$

where $\mathbf{Q} \equiv (\mathbf{R}, \mathbf{P})$ and $\mathbf{q} \equiv (\mathbf{r}^N, \mathbf{p}^N)$.

Now, we introduce the following fluid molecule conditional distribution function

$$h(\mathbf{q}, t; \mathbf{Q}, t) = \frac{f(\mathbf{q}, \mathbf{Q}, \mathbf{t})}{\Psi(\mathbf{Q}, t)} \tag{27}$$

The *actual* initial state for f can then be written in terms of the multiple time scales as

$$f(\mathbf{q}, 0, 0,...) = h(\mathbf{q}, 0, 0,...; \mathbf{Q}, 0, 0,...)\ \Psi(\mathbf{Q}, 0, 0,...) \tag{28}$$

For example, a common initial state in Brownian dynamics simulations is for the position and momentum of the particle to be known at time $t = 0$, i.e.,

$$\Psi(\mathbf{Q}, 0, 0, 0) = \delta(\mathbf{Q} - \mathbf{Q}_0) \tag{29}$$

and for the fluid molecules to have established an equilibrium state in the potential field of the particle and, in our case, the wall, i.e.,

$$h(\mathbf{q}, 0, 0,...; \mathbf{Q}, 0, 0, 0) = h_{eq} \tag{30}$$

where h_{eq} follows from the solution to

$$L_f h_{eq} = 0 \tag{31}$$

Looking at Eq. (11), it is clear that this "rapid relaxation" of the fluid depends on the Knudsen number for any particular system with γ small. Here, we will assume that the Knudsen number is always small enough such that the "rapid relaxation" assumption is valid. More discussion on the effects of initial conditions will be given later [also, see reference 8], however, we note that the general behavior of $h^{(0)} \equiv f^{(0)}/\Psi^{(0)}$ on the τ_0 time scale is given by Eqs. (25) and (26) as

$$\frac{\partial h^{(0)}}{\partial \tau_0} = -N_{\mathrm{Kn}}^{-1} L_f h^{(0)} \tag{32}$$

or

$$h^{(0)} = e^{-N_{\mathrm{Kn}}^{-1} L_f \tau_0} h^{(0)}(\mathbf{q}, 0, \tau_1,...; \mathbf{Q}, 0, \tau_1,...) \tag{33}$$

Now, analogizing the remarks of Piasecki[6] in the case of the Lorentz electron gas, it is convenient but not necessary to choose the initial state of $f^{(0)}(\mathbf{q}, \mathbf{Q}, 0, \tau_1, \tau_2,...)$ to be given, in part, by the actual initial equilibrium state for the fluid [from Eq. (30)], i.e.,

$$\begin{aligned} f^{(0)}(\mathbf{q}, \mathbf{Q}, 0, \tau_1, \tau_2,...) &= h^{(0)}(\mathbf{q}, 0, \tau_1,...; \mathbf{Q}, 0, \tau_1,...)\ \Psi^{(0)}(\mathbf{Q}, 0, \tau_1, \tau_2,...) \\ &= h_{eq}\, \Psi^{(0)}(\mathbf{Q}, \tau_1, \tau_2,...) \end{aligned} \tag{34}$$

We also choose

$$f^{(n)}(\mathbf{q}, \mathbf{Q}, 0, \tau_1, \tau_2, \ldots) = 0, \qquad n \geqslant 1 \tag{35}$$

and

$$\Psi^{(n)}(\mathbf{Q}, 0, \tau_1, \tau_2, \ldots) = 0, \qquad n \geqslant 1 \tag{36}$$

Now with the initial state given by Eq. (34), it follows from Eq. (26) that

$$f^{(0)}(\mathbf{q}, \mathbf{Q}, \tau_0, \tau_1, \ldots) = f^{(0)}(\mathbf{q}, \mathbf{Q}, \tau_1, \ldots) = h_{eq}\, \Psi^{(0)}(\mathbf{Q}, \tau_1, \tau_2, \ldots) \tag{37}$$

Also,

$$\mathscr{L} f^{(0)} = \frac{\partial \Psi^{(0)}}{\partial \mathbf{P}} \cdot \int h_{eq} \frac{\partial}{\partial \mathbf{R}} \sum_{i=1}^{N} u_{fp}(\mathbf{r}_i - \mathbf{R})\, d\mathbf{r}^N\, d\mathbf{p}^N \tag{38}$$

where h_{eq} is assumed not to depend on the given particle momentum at time $t = 0$. (See Eqs. (47)–(49) below.)

Introducing an equilibrium average force exerted on the particle by the fluid

$$\langle \mathbf{F}_f \rangle_{eq} = -\int h_{eq} \frac{\partial}{\partial \mathbf{R}} \sum_{i=1}^{N} u_{fp}(\mathbf{r}_i - \mathbf{R})\, d\mathbf{r}^N\, d\mathbf{p}^N \tag{39}$$

we obtain

$$\mathscr{L} f^{(0)} = -\frac{\partial \Psi^{(0)}}{\partial \mathbf{P}} \cdot \langle \mathbf{F}_f \rangle_{eq} \tag{40}$$

Now, in the absence of wall effects, it is justifiable to assume that the equilibrium average force on the particle is zero. However, a careful analysis shows that h_{eq} depends not only on the potential between the fluid and particle, but also depends on the potential between the fluid and wall [see L_f expression, Eq. (12)]. Therefore, in general, $\langle \mathbf{F}_f \rangle_{eq} \neq 0$ in the presence of a wall.

Having determined $\mathscr{L} f^{(0)}$, we can solve Eq. (23), with the initial state Eq. (36), as

$$\Psi^{(1)}(\mathbf{Q}, \tau_0, \tau_1, \ldots) = \tau_0 \left[-\mathbf{P} \cdot \frac{\partial \Psi^{(0)}}{\partial \mathbf{R}} + \frac{\partial u_{pw}}{\partial \mathbf{R}} \cdot \frac{\partial \Psi^{(0)}}{\partial \mathbf{P}} - \langle \mathbf{F}_f \rangle_{eq} \cdot \frac{\partial \Psi^{(0)}}{\partial \mathbf{P}} - \frac{\partial \Psi^{(0)}}{\partial \tau_1} \right] \tag{41}$$

From this equation it is seen that $\Psi^{(1)}$ grows unbounded with τ_0 (secular behavior) unless

$$\frac{\partial \Psi^{(0)}}{\partial \tau_1} = \left\{ -\mathbf{P} \cdot \frac{\partial \Psi^{(0)}}{\partial \mathbf{R}} - \left[\langle \mathbf{F}_f \rangle_{eq} - \frac{\partial u_{pw}}{\partial \mathbf{R}} \right] \cdot \frac{\partial \Psi^{(0)}}{\partial \mathbf{P}} \right\} \tag{42}$$

The above equation describes the leading-order behavior of $\Psi^{(0)}$ on the τ_1 time scale. Note that we also have upon eliminating secular behavior

$$\Psi^{(1)}(\mathbf{Q}, \tau_0, \tau_1, \ldots) = 0 \tag{43}$$

In order to proceed further, we must determine the behavior of $f^{(1)}$ according to Eq. (20). In a general way, Eq. (20) can be integrated to give

$$f^{(1)} = -\int_0^{\tau_0} e^{-N_{\mathrm{Kn}}^{-1} L_f s} \left[\frac{\partial f^{(0)}}{\partial \tau_1} + L_p f^{(0)} \right] ds \tag{44}$$

where $f^{(1)}(\mathbf{q}, \mathbf{Q}, 0, \tau_1, \ldots) = 0$. Using $f^{(0)} = h_{eq} \Psi^{(0)}$ along with Eqs. (13) and (42) yields

$$f^{(1)} = -\int_0^{\tau_0} e^{-N_{\mathrm{Kn}}^{-1} L_f s} \left\{ \Psi^{(0)} \left[\mathbf{P} \cdot \frac{\partial h_{eq}}{\partial \mathbf{R}} + \left(\mathbf{F}_f - \frac{\partial u_{pw}}{\partial \mathbf{R}} \right) \cdot \frac{\partial h_{eq}}{\partial \mathbf{P}} \right] + \frac{\partial \Psi^{(0)}}{\partial \mathbf{P}} \cdot h_{eq} (\mathbf{F}_f - \langle \mathbf{F}_f \rangle_{eq}) \right\} ds \tag{45}$$

where

$$\mathbf{F}_f \equiv -\frac{\partial}{\partial \mathbf{R}} \left[\sum_{i=1}^{N} u_{fp}(\mathbf{r}_i - \mathbf{R}) \right] \tag{46}$$

Now we must specify the general functional form of h_{eq}. For *global* equilibrium, h_{eq} follows from the separable solution to $L_f h_{eq} = 0$, i.e.,

$$h_{eq} = \frac{\exp[-H_f]}{\iint \exp[-H_f] \, d\mathbf{r}^N \, d\mathbf{p}^N} \tag{47}$$

where H_f is the dimensionless Hamiltonian for the fluid molecules in the presence of the particle and the wall,

$$H_f = \sum_{i=1}^{N} \left[p_i^2 + \sum_{j,\, j<i} u_{ff}(\mathbf{r}_i - \mathbf{r}_j) + u_{fp}(\mathbf{r}_i - \mathbf{R}) + u_{fw}(\mathbf{r}_i - \mathbf{R}_w) \right] \tag{48}$$

Thus,

$$\frac{\partial h_{eq}}{\partial \mathbf{P}} = 0, \qquad \text{global equilibrium} \tag{49}$$

and

$$\frac{\partial h_{eq}}{\partial \mathbf{R}} = h_{eq}(\mathbf{F}_f - \langle \mathbf{F}_f \rangle_{eq}), \qquad \text{global equilibrium} \tag{50}$$

Other solutions to $h^{(0)}$ have also been conjectured based on *local* equilibrium conditions.[9] As pointed out by Mazo,[9] however, neither local equilibrium or global equilibrium addresses the effects of the initial state as discussed previously. Our interest here is on the effects of a wall and we will assume global equilibrium on the τ_0 time scale to hold. Specific molecular dynamics results will also be given below in order to examine this assumed behavior.

Thus, we have from Eqs. (45), (49), and (50) that

$$f^{(1)} = -\left(\Psi^{(0)}\mathbf{P} + \frac{\partial}{\partial \mathbf{P}} \Psi^{(0)} \right) \cdot \int_0^{\tau_0} h_{eq} e^{-N_{\mathrm{Kn}}^{-1} L_f s} (\mathbf{F}_f - \langle \mathbf{F}_f \rangle_{eq})\, ds \tag{51}$$

Now, integrating Eq. (24), with $\Psi^{(1)} = 0$ and $\Psi^{(2)}(\mathbf{Q}, 0, \tau_1, \ldots) = 0$,

$$\Psi^{(2)}(\mathbf{Q}, \tau_0, \tau_1, \ldots) = -\tau_0 \frac{\partial \Psi^{(0)}}{\partial \tau_2} + \int_0^{\tau_0} \mathscr{L} f^{(1)}(\mathbf{q}, \mathbf{Q}, x, \tau_1, \ldots)\, dx \tag{52}$$

The integral term is given explicitly by

$$\begin{aligned}
&\int_0^{\tau_0} \mathscr{L} f^{(1)}(\mathbf{q}, \mathbf{Q}, x, \tau_1, \ldots)\, dx \\
&\quad = \int_0^{\tau_0} \left\{ \int_{\mathbf{r}^N,\, \mathbf{p}^N} \mathbf{F}_f \cdot \frac{\partial}{\partial \mathbf{P}} \left(\Psi^{(0)}\mathbf{P} + \frac{\partial \Psi^{(0)}}{\partial \mathbf{P}} \right) \right. \\
&\qquad \left. \cdot \left[\int_0^x h_{eq} e^{-N_{\mathrm{Kn}}^{-1} L_f s} (\mathbf{F}_f - \langle \mathbf{F}_f \rangle_{eq})\, ds \right] d\mathbf{r}^N\, d\mathbf{p}^N \right\} dx \\
&\quad = \frac{\partial}{\partial \mathbf{P}} \cdot \int_0^{\tau_0} \left\{ \int_{\mathbf{r}^N,\, \mathbf{p}^N} h_{eq} \mathbf{F}_f \left[\int_0^x e^{-N_{\mathrm{Kn}}^{-1} L_f s} (\mathbf{F}_f - \langle \mathbf{F}_f \rangle_{eq})\, ds \right] d\mathbf{r}^N\, d\mathbf{p}^N \right\} dx \\
&\qquad \cdot \left(\Psi^{(0)}\mathbf{P} + \frac{\partial \Psi^{(0)}}{\partial \mathbf{P}} \right)
\end{aligned} \tag{53}$$

Noting that $\mathbf{F}_f$ and L_f do not depend explicitly on time, we can rewrite the above equation as

$$\int_0^{\tau_0} \mathscr{L} f^{(1)}(\mathbf{q}, \mathbf{Q}, x, \tau_1, \ldots)\, dx = \frac{\partial}{\partial \mathbf{P}} \cdot \int_0^{\tau_0} \int_0^x \langle \mathbf{F}_f [e^{-N_{\mathrm{Kn}}^{-1} L_f s} (\mathbf{F}_f - \langle \mathbf{F}_f \rangle_{eq})] \rangle_{eq}\, ds\, dx \cdot \left(\Psi^{(0)} \mathbf{P} + \frac{\partial \Psi^{(0)}}{\partial \mathbf{P}} \right) \tag{54}$$

Interchanging the order of the time integrations gives

$$\int_0^{\tau_0} \mathscr{L} f^{(1)}(\mathbf{q}, \mathbf{Q}, x, \tau_1, \ldots)\, dx = \frac{\partial}{\partial \mathbf{P}} \cdot \tau_0 \int_0^{\tau_0} \left(1 - \frac{s}{\tau_0}\right) \langle \mathbf{F}_f(0) [\mathbf{F}_f(-s) - \langle \mathbf{F}_f \rangle_{eq}] \rangle_{eq}\, ds \cdot \left(\Psi^{(0)} \mathbf{P} + \frac{\partial \Psi^{(0)}}{\partial \mathbf{P}} \right) \tag{55}$$

where we have introduced

$$\mathbf{F}_f(-s) \equiv e^{-N_{\mathrm{Kn}}^{-1} L_f s} \mathbf{F}_f \tag{56}$$

which represents the value of $\mathbf{F}_f$ at some point in time, $-s$, beginning with an initial value of $\mathbf{F}_f(0)$ (see Appendix).

Note, importantly, that the particle coordinates, $\mathbf{Q}$, are to be kept fixed in evaluating the time integral in Eq. (55) according to the operator L_f.

Returning to Eq. (52), in order to remove secular behavior we must have

$$\frac{\partial \Psi^{(0)}}{\partial \tau_2} = \lim_{\tau_0 \to \infty} \frac{\partial}{\partial \mathbf{P}} \cdot \int_0^{\tau_0} \left(1 - \frac{s}{\tau_0}\right) \langle \mathbf{F}_f(0) [\mathbf{F}_f(-s) - \langle \mathbf{F}_f \rangle_{eq}] \rangle_{eq}\, ds \cdot \left(\Psi^{(0)} \mathbf{P} + \frac{\partial \Psi^{(0)}}{\partial \mathbf{P}} \right) \tag{57}$$

and also then

$$\Psi^{(2)} = 0 \tag{58}$$

We note that, as given by Eq. (A2), $\mathbf{F}_f(-s)$ is subject to the same dynamical conditions as $h^{(0)}$ from Eq. (32), i.e., the rapid relaxation

assumption with $N_{\mathbf{Kn}} \ll 1$. Thus, with this consistently applied assumption the correlation function $\langle \mathbf{F}_f(0)\, \mathbf{F}_f(-s) \rangle_{eq}$ must decay rapidly to $\langle \mathbf{F}_f \rangle_{eq}^2$ on the τ_0 time scale. Importantly, if the rapid relaxation assumption does not hold for $\mathbf{F}_f(-s)$, then it does not hold for $h^{(0)}$ either. Further analysis and verification will be made when molecular dynamics results are presented; we also refer the interested reader to reference[8] for more discussion.[2] Returning to Eq. (57), we can write

$$\frac{\partial \Psi^{(0)}}{\partial \tau_2} = \frac{\partial}{\partial \mathbf{P}} \cdot \zeta \cdot \left(\Psi^{(0)} \mathbf{P} + \frac{\partial \Psi^{(0)}}{\partial \mathbf{P}} \right) \tag{59}$$

where the time-independent friction tensor, τ, is given by[3]

$$\zeta \equiv \int_0^\infty [\langle \mathbf{F}_f(0)\, \mathbf{F}_f(-s) \rangle_{eq} - \langle \mathbf{F}_f \rangle_{eq}^2]\, ds \tag{60}$$

In the absence of wall effects, we have the well-known results

$$\zeta = \int_0^\infty \langle \mathbf{F}_f(0)\, \mathbf{F}_f(-s) \rangle_{eq}\, ds \tag{61}$$

Note that because of the time reversal behavior of the "microscopic" equations, the force correlation functions are symmetric in time, i.e.,

$$\langle \mathbf{F}_f(0)\, \mathbf{F}_f(-s) \rangle = \langle \mathbf{F}_f(0)\, \mathbf{F}_f(s) \rangle \tag{62}$$

Summarizing, up to the τ_2 time scale, we have

$$\begin{aligned} \frac{\partial \Psi}{\partial t} &= \frac{\partial \Psi^{(0)}}{\partial \tau_0} + \gamma \frac{\partial \Psi^{(0)}}{\partial \tau_1} + \gamma^2 \frac{\partial \Psi^{(0)}}{\partial \tau_2} + 0(\gamma^3) \\ &= \gamma \left\{ -\mathbf{P} \cdot \frac{\partial \Psi^{(0)}}{\partial \mathbf{R}} - \left[\langle \mathbf{F}_f \rangle_{eq} - \frac{\partial u_{pw}}{\partial \mathbf{R}} \right] \cdot \frac{\partial \Psi^{(0)}}{\partial \mathbf{P}} \right\} \\ &\quad + \gamma^2 \left[\frac{\partial}{\partial \mathbf{P}} \cdot \zeta \cdot \left(\Psi^{(0)} \mathbf{P} + \frac{\partial \Psi^{(0)}}{\partial \mathbf{P}} \right) \right] \end{aligned} \tag{63}$$

[2] For a recent treatment of molecular friction in a dense gas, see L. Bocquet, J. Piasecki, and J.-P. Hansen, *J. Stat. Phys.* **76**:505–548 (1994). An anomalous case is that of a free-molecule gas, which by definition has no "memory" effects and Eqs. (60) and (61) hold for this case as well.[3]

[3] Note that Eq. (60) needs to be interpreted carefully; the result only follows for $N_{\mathbf{Kn}} \ll 1$, i.e., the "rapid relaxation" assumption. The analysis here shows that Eqs. (60) or (61) should not be stated without this qualification, as sometimes has been done. [See P. Español and I. Zuñiga, *J. Chem. Phys.* **98**:574–580 (1993).]

or, since $\Psi = \Psi^{(0)} + \gamma\Psi^{(1)} + \gamma^2\Psi^{(2)} + \cdots$, and $\Psi^{(1)} = \Psi^{(2)} = 0$, we finally obtain the Fokker–Planck (FP) equation for a particle near a wall as

$$\frac{\partial \Psi}{\partial t} + \gamma \mathbf{P} \cdot \frac{\partial \Psi}{\partial \mathbf{R}} + \gamma \left[\langle \mathbf{F}_f \rangle_{eq} - \frac{\partial u_{pw}}{\partial \mathbf{R}} \right] \cdot \frac{\partial \Psi}{\partial \mathbf{P}} = \gamma^2 \left[\frac{\partial}{\partial \mathbf{P}} \cdot \zeta \cdot \left(\Psi \mathbf{P} + \frac{\partial \Psi}{\partial \mathbf{P}} \right) \right] + 0(\gamma^3) \tag{64}$$

where the friction tensor is given by Eq. (60). Note that both γ and N_{Kn} are considered small. In terms of dimensional variables, the FP equation reads

$$\frac{\partial \Psi}{\partial t} + \frac{\mathbf{P}}{M} \cdot \frac{\partial \Psi}{\partial \mathbf{R}} + \left[\langle \mathbf{F}_f \rangle_{eq} - \frac{\partial u_{pw}}{\partial \mathbf{R}} \right] \cdot \frac{\partial \Psi}{\partial \mathbf{P}} = kT \left\{ \frac{\partial}{\partial \mathbf{P}} \cdot \zeta \cdot \left[\Psi \frac{\mathbf{P}}{MkT} + \frac{\partial \Psi}{\partial \mathbf{P}} \right] \right\} \tag{65}$$

where

$$\zeta \equiv \frac{1}{kT} \int_0^\infty \left[\langle \mathbf{F}_f(s)\, \mathbf{F}_f(0) \rangle_{eq} - \langle \mathbf{F}_f \rangle_{eq}^2 \right] ds \tag{66}$$

In what follows, we do not attempt to develop analytical expressions for Eq. (66) based on, for example, continuum hydrodynamic theories [see, e.g., ref. 10]. Numerically, the FP equation can be solved discretely for small time steps [the Brownian dynamics (BD) method], where the particle force parameters $\langle \mathbf{F}_f \rangle_{eq}$, $\partial u_{pw}/\partial \mathbf{R}$, and ζ are assumed constant over each time step.[11] At the beginning of each BD time step, equilibrium molecular dynamics simulations can be conducted in order to determine $\langle \mathbf{F}_f \rangle_{eq}$, and ζ. In doing this, we avoid the restrictive assumptions of an analytical theory as discussed in the Introduction section of this paper. Also, note that since we have assumed global equilibrium, the molecular dynamics (MD) algorithm is a well-known canonical equilibrium algorithm, [cf. Eq. (47)] and therefore straightforward to apply. The MD algorithm is only applied at the beginning of each BD time step, and thus long-time dynamics of particles can be probed that are not currently possible by MD algorithms alone.

3. MOLECULAR DYNAMICS SIMULATIONS AND THE FORCE AUTOCORRELATION FUNCTION

As noted above, the force autocorrelation function (FAF) can be obtained by conducting standard canonical, equilibrium molecular

dynamics simulations. Note again that the particle phase space coordinates are to be held fixed, according to Eq. (56), in the FAF analysis. Also, the FAF must decay rapidly over the τ_0 time scale, which requires $N_{\mathrm{Kn}} \ll 1$. This restricts the theory to the liquid regime for the fluid. No attempt is made here to review all aspects of equilibrium molecular dynamics as these are well described in many texts [see, e.g., refs. 12–14]. Briefly, all results reported here were based on the use of the Verlett algorithm and velocity rescaling methods to maintain isothermal conditions.[12] In order to test the method, simple systems consisting of (A) a single spherical particle with no external surface present and (B) a single particle near an external spherical surface were analyzed and compared to known analytical results as discussed below. The only MD simulation anomaly pertains to the use of minimum image conventioning in that the MD cell containing the particle must be large enough to avoid "image" particle effects. Cell size specifications are listed for all simulation results below.

A. Single Spherical Particle Results

A typical molecular dynamics simulation for a single spherical particle in a molecular fluid is graphically illustrated in Fig. 1. Two types of molecule-particle force interactions were investigated. In the first type, a simple Lennard–Jones interaction potential was used as given by

$$u(r) = 4\varepsilon' \left[\left(\frac{\sigma'}{r} \right)^{12} - \left(\frac{\sigma'}{r} \right)^{6} \right] \tag{67}$$

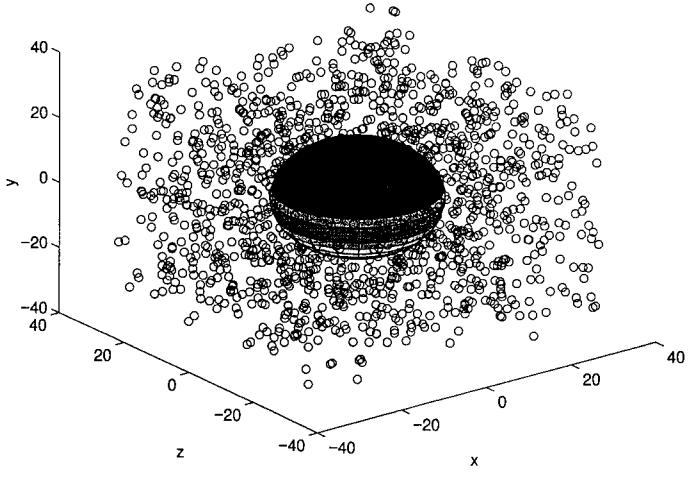

Fig. 1. Illustration of the molecular dynamics simulation in single sphere systems.

where $\varepsilon' = (\varepsilon_s \varepsilon_m)^{1/2}$, $\sigma' = (\sigma + d)/2$, ε_s is a L–J potential constant for the spherical particle (treated as a larger molecule), ε_m is a L–J potential constant for the fluid molecule, σ is the molecule diameter, d is the particle diameter, and r is the separation distance between the molecule and the particle center. A typical potential and force predicted from Eq. (67) is shown in Fig. 2.

In the second type, the spherical particle was considered to be composed of a large number of molecules each interacting with the fluid molecules according to a Lennard–Jones potential. The potential energy of interaction between a single fluid molecule and the molecular aggregate sphere can be obtained by integrating (summing) over the entire volume of the sphere. It can readily be shown that this results in the following expression for the potential

$$u(r) = q \frac{\varepsilon \pi \sigma^6}{3r} \left\{ \frac{\sigma^6}{30} \left[\frac{(r+9r_s)}{(r+r_s)^9} - \frac{(r-9r_s)}{(r-r_s)^9} \right] - \left[\frac{(r+3r_s)}{(r+r_s)^3} - \frac{(r-3r_s)}{(r-r_s)^3} \right] \right\} \tag{68}$$

where q is the number of molecules per unit volume of the sphere, ε is a L–J interaction potential constant for a fluid molecule–particle molecule interaction (assumed equal), r_s is the particle radius, and r is the separation distance between the molecule and center of mass of the particle.

A typical potential and force determined from Eq. (68) is shown in Fig. 3. For either type of potential, an effective particle radius is selected by the usual prescription of the location in the zero of the potential (see

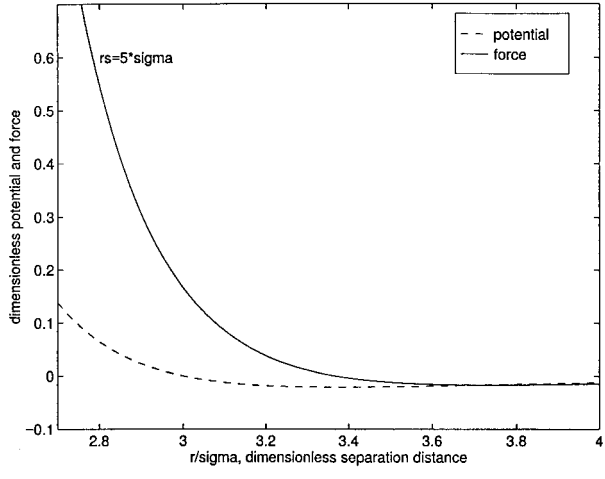

Fig. 2. Illustration of the interaction potential and force for a simple Lennard–Jones interaction between a fluid molecule and a spherical particle treated as a larger molecule.

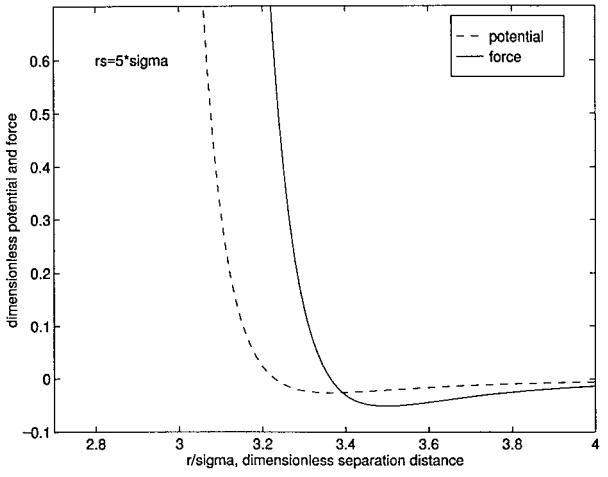

Fig. 3. Illustration of the interaction potential and force for the "integrated" or summed Lennard–Jones interaction between a fluid molecule and a spherical particle composed of molecules in an FCC arrangement.

Table 1. MD Simulation Parameters for Simple LJ Interaction[a]

Particle diameter/σ	Effective diameter/σ	Control box length, l/σ	$N = \rho^*(l^3 - \frac{1}{6}\pi d_{eff}^3)$, number of fluid molecules
2.5	3.5	10	708
3.75	4.75	10	684
5.0	6.0	10	643
6.25	7.25	12	1108

[a] Fluid parameters: $T^* = T/(\varepsilon/k) = 1.0017$, $\rho^* = 0.725$. Time step: $\Delta t = 0.5 \times 10^{-14}$ sec. Total time steps: 60,000–80,000.

Table 2. MD Simulation Parameters for Integrated LJ Interaction[a]

Particle diameter/σ	Effective diameter/σ	Control box length, l/σ	$N = \rho^*(l^3 - \frac{1}{6}\pi d_{eff}^3)$, number of fluid molecules
2.5	3.99	10	700
3.75	5.23	10	670
5.0	6.46	11	863
6.25	7.72	12	1078

[a] Fluid parameters: $T^* = T/(\varepsilon/k) = 1.0017$, $\rho^* = 0.725$. Time step: $\Delta t = 1.0 \times 10^{-15}$ sec. Total time steps: 60,000–80,000.

Tables 1 and 2). For the fluid-fluid interactions, a simple Lennard–Jones potential was also used.

For the purposes of simulation, values for Argon were used to select all potential parameters ($\varepsilon/k = 119.8K$, $\sigma = 3.405A$, and $m = 6.63382 \times 10^{-26}kg$). Thus, we investigated solid Argon spheres in an Argon fluid assuming no condensation or evaporation along the phase boundary. Solid Argon is known to assume an fcc structure with $q = \sqrt{2}/r_{\min}^3$, where $r_{\min} = 1.12246\sigma$.[15]

Figure 4 shows a typical particle force autocorrelation function obtained with the fluid in the liquid regime for a simple Lennard–Jones interaction [Eq. (67)]. The specific simulation parameters are given in Table 1. Figure 5 shows a typical force autocorrelation function obtained for the integrated L–J potential. The specific simulation parameters are given in Table 2 for this case. Note that the force correlation values shown in Figs. 5 and 6 are based on averaging over fifteen to twenty separate intervals. Standard deviations from the fifteen to twenty samples are also shown in Figs. 5 and 6. Standard deviations can be reduced by increasing the total simulation time, but this generally requires larger systems to avoid periodicity effects.[14]

In Figs. 6 and 7, the diagonal friction tensor components are shown for the two potential types as determined from Eq. (65), using the average force correlation values from Figs. 5 and 6, along with the prediction of

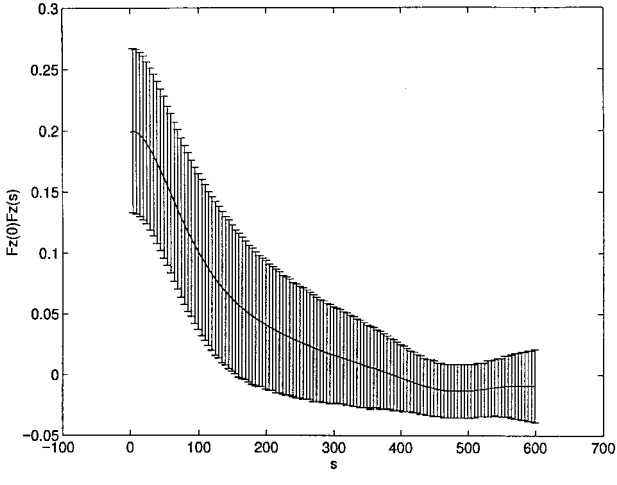

Fig. 4. Typical force autocorrelation function for the simple LJ interaction. Note that the ford and time shown are dimensionless using the characteristic force as $48\varepsilon/\sigma$ and the characteristic time as $[m\sigma^2/(48\varepsilon)]^{1/2}$.

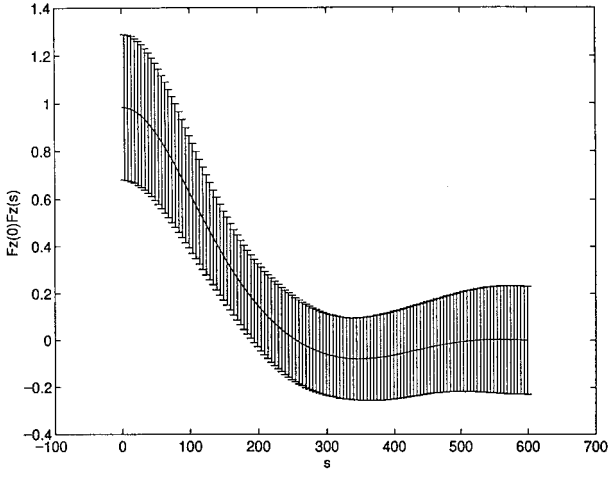

Fig. 5. Typical force autocorrelation function for the integrated LJ potential. Note that the force and time shown are dimensionless using the characteristic force as $48\varepsilon/\sigma$ and the characteristic time as $[m\sigma^2/(48\varepsilon)]^{1/2}$.

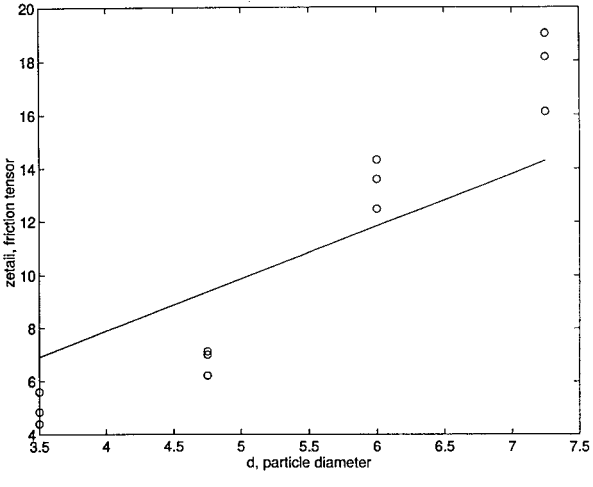

Fig. 6. Diagonal components of the friction tensor ($ii = xx$, yy, or zz) computed from the force autocorrelation function for the simple LJ interaction. Also shown is Stokes' law prediction using an effective particle radius (see Table 1). The friction tensor shown is dimensionless using the characteristic value of $[\sigma^2/(48\varepsilon)]^{1/2}$.

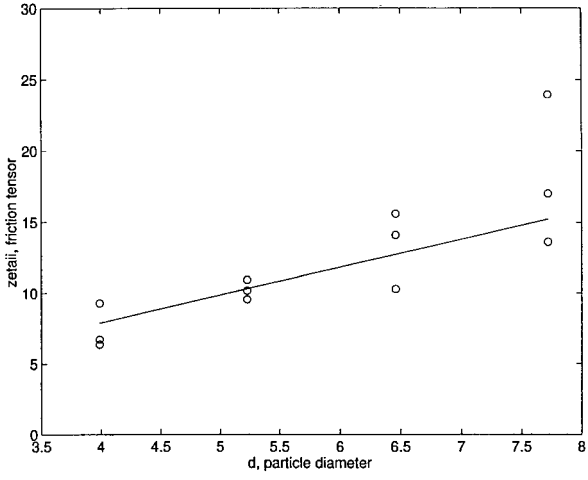

Fig. 7. Diagonal components of the friction tensor computed from the force autocorrelation function for the integrated LJ interaction. Also shown is Stokes' law prediction using an effective particle radius (see Table 2). The friction tensor shown is dimensionless using the characteristic value of $[\sigma^2/(48\varepsilon)]^{1/2}$.

Stokes' law using the effective sphere radius and tabulated (physical) experimental values for the viscosity of argon (CRC Handbook of Chemistry and Physics, 77th edition) ($\zeta_{Stokes} = 6\pi\mu r_{eff}$). As can be seen very good agreement is obtained. Note that for the smallest diameter systems shown, no attempt was made to use generalized hydrodynamics[16] for comparison purposes due to the scatter present.

We also examined the effects of the thermostat on the friction tensor calculations. As discussed above, a velocity rescaling method was used in order to maintain isothermal conditions; the molecular velocities are rescaled every time step. One way to examine the *sensitivity* of the results on the thermostat conditions can be accomplished by varying the time interval for rescaling of the velocities. Figure 8 shows the friction tensor as a function of the velocity rescaling time interval. As can be seen, rescaling the velocity every one to five steps has no measurable effect on the results. This is due to the extremely small change in the total molecular kinetic energy over these time steps ($< 1\%$). As shown in Fig. 8, we must go as large as rescaling every ten time steps in order to observe spurious behavior of the friction tensor calculations. In these extreme cases, the total kinetic energy changes are large enough to significantly perturb the molecular velocities during rescaling. We conclude that the force autocorrelation calculations are somewhat insensitive to the manner of maintaining the thermostat.

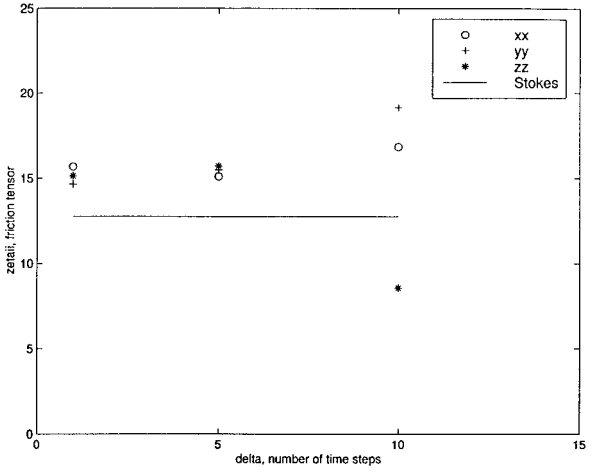

Fig. 8. Diagonal components of the friction tensor ($ii = xx$, yy, or zz) as a function of the number of time steps between velocity resealing for the integrated LJ interaction. The particle diameter is 5σ.

Interestingly, it is to be noted that the ILJ potential results in larger values of the static force correlation $\langle \mathbf{F}(0)\,\mathbf{F}(0)\rangle$ and more rapid decay than the simple LJ. Thus, the integral of the force correlation over time, which is proportional to the friction tensor, becomes nearly independent of the type of potential provided that the effective sphere diameters are employed. This result is in agreement with previous studies in single sphere systems.[16]

Further analysis of the static force correlation can also be shown to be useful. Following Boon and Yip,[17] the static force correlation can be separated into binary and three-body interactions as

$$\langle \mathbf{F}(0)\,\mathbf{F}(0)\rangle_{eq} = \left\langle \sum_{i=1}^{N} \mathbf{F}_{oi}\mathbf{F}_{oi} \right\rangle_{eq} + \left\langle \sum_{i=1}^{N} \sum_{\substack{j=1 \\ j\neq i}}^{N} \mathbf{F}_{oi}\mathbf{F}_{oj} \right\rangle_{eq}$$

$$= \mathbf{F}_2^2(0) + \mathbf{F}_3^2(0) \tag{69}$$

where $\mathbf{F}_{oi}$ is the force exerted on spherical particle by molecule i at time $t = 0$. Again, following Boon and Yip,[17] it can be shown that the two-body, $\mathbf{F}_2^2(0)$, and three-body, $\mathbf{F}_3^2(0)$, terms can be expressed in terms of the single molecule-particle radial distribution function and its gradient as

$$F^2_{2_{ii}}(0) = \frac{4\pi n}{3} \int r^2 g(r) \left[\frac{du(r)}{dr} \right]^2 dr \tag{70}$$

$$F^2_{3_{ii}}(0) = \frac{4}{3} \pi n (kT)^2 \int r^2 \left\{ -\frac{1}{kT} \frac{du(r)}{dr} \frac{dg(r)}{dr} - \frac{1}{(kT)^2} g(r) \left[\frac{du(r)}{dr} \right]^2 \right\} dr \tag{71}$$

$ii = xx$, yy, or zz in Cartesian coordinates with all off diagonal terms being zero. Combining Eqs. (70) and (71) we obtain

$$\langle F^2_{ii}(0) \rangle_{eq} = -\frac{4}{3} \pi n k T \int r^2 \left[\frac{du(r)}{dr} \frac{dg(r)}{dr} \right] dr \tag{72}$$

Note that Eq. (70) is dominant in rarefied gases with $F^2_{3ii}(0) = 0$, i.e., no three-body interactions (fluid molecule–fluid molecule–partible). For "hard" interactions in a rarefied gas system, following Boon and Yip,[17] an estimate of the static force correlation is

$$F^2_{2ii}(0) = \tfrac{4}{3} \pi n \beta^{-2} \sigma_e \, y(\sigma_e) \, \Lambda_e \tag{73}$$

where n is the number density of the liquid, $\beta = (1/kT)$, σ_e is the effective sphere diameter, $y(r)$ is the Mayer function,

$$y(r) \equiv g(r) \exp[\beta u(r)] \tag{74}$$

and Λ_e is a hardness index. For a rarefied gas $y(\sigma_e) = 1$ and for the simple L–J interaction $\Lambda_e = 12$. The decay time can be estimated as[17]

$$t_d = \frac{\sigma_e}{\Lambda_e v_o} \tag{75}$$

where v_o is a characteristic velocity of the molecule-particle encounter. Using the mean molecular speed $[v_o = (8kT/\pi m)^{1/2}]$, and assuming a simple linear decay, leads to an estimate of the friction tensor for a highly dilute gas (no fluid molecular interactions) as

$$\zeta = 4.188 n (2\pi m k T)^{1/2} r^2_{eff} \tag{76}$$

which compares well with Epstein's classical formula for a spherical particle with specular reflection boundary conditions[18]

$$\zeta = \tfrac{8}{3} n (2\pi m k T)^{1/2} r^2_{eff} \tag{77}$$

In the more general case, in order to estimate the two- and three-body contributions to the static force correlation, the radial distribution function

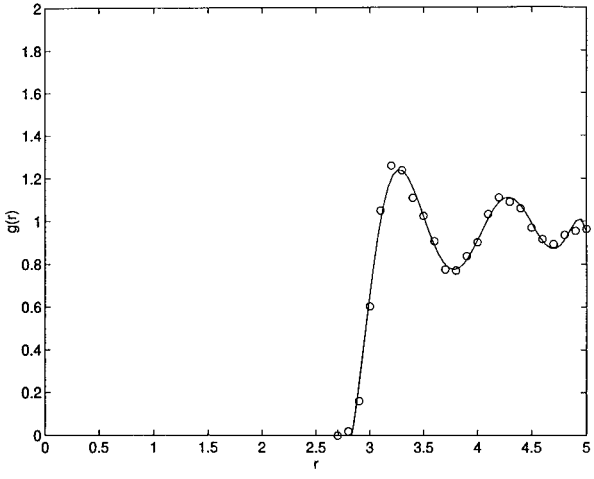

Fig. 9. Typical radial distribution function for the simple LJ interaction potential.

and its gradient are needed. This can be obtained experimentally, from molecular dynamics or from, e.g., the hypernetted chain equation.[19] Figures 9 and 10 show typical radial distribution functions obtained from molecular dynamics for the simple L–J system and the integrated L–J system, respectively. Note that a much larger first coordination shell density is exhibited for the integrated L–J system due to its deeper potential

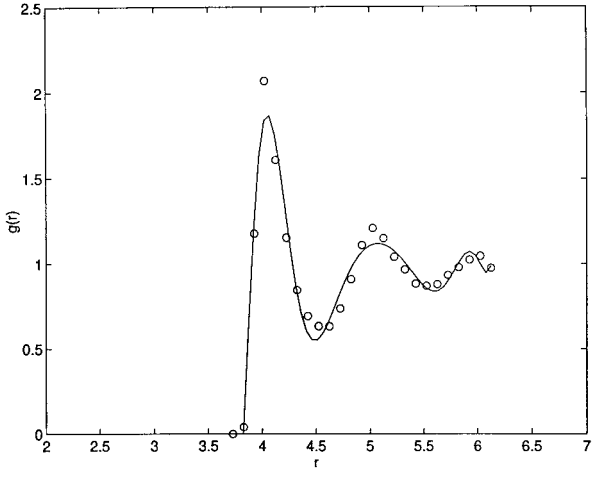

Fig. 10. Typical radial distribution function for the integrated LJ interaction potential.

Table 3. Comparison of the Static Force Correlation Function Calculated from Theory [Eq. (76)] and Directly from Experiments (Molecular Dynamics)[a]

Potential type	Diameter/σ	d_{eff}/σ	$\langle F_i^2(0)\rangle_{\text{theory}}$	$\langle F_i^2(0)\rangle_{\text{exp}}$
LJ	1.0	2.0	0.092	0.105
LJ	5.0	6.0	0.160	0.167
ILJ	6.25	7.72	1.169	1.122

[a] For other simulation parameters, please refer to Tables 1 and 2.

minimum. In Table 3, calculations of the static force correlation from Eq. (72) show excellent agreement with the static force values obtained directly from simulation in the liquid regime for both potential types.

B. Single Spherical Particle near an External Spherical Surface (Adsorbate)

Because of the availability of analytical results for the hydrodynamic interactions of two spheres, a number of simulations were carried out for this type of system. The Cartesian components of the friction tensor for a single spherical Brownian particle near a fixed external sphere (adsorbate or "collector") is given to $\tilde{O}(1/R^6)$ by ref. 11.

$$\zeta_{zz} = 6\pi\mu r_s \left[1 + \frac{9}{4}\frac{r_s b}{R^2} - \frac{3r_s b(r_s^2 + b^2)}{2R^4} + \frac{15}{4}\frac{r_s b^3}{R^4} + \frac{81}{16}\frac{r_s^2 b^2}{R^4} \right] \tag{78}$$

$$\zeta_{xx} = \zeta_{yy} = 6\pi\mu r_s \left[1 + \frac{9}{16}\frac{r_s b}{R^2} + \frac{9}{4}\frac{r_s b(r_s^2 + b^2)}{R^4} + \frac{81}{256}\frac{r_s^2 b^2}{R^4} \right] \tag{79}$$

where the z-axis is along line of centers of the particle and the external sphere, r_s is the particle radius, b is the external sphere radius, and R is the separation distance. All off-diagonal elements of the friction tensor are zero for this case.[11] Higher-order approximations to Eqs. (78) and (79) are also available,[11, 20] however, as will be shown, these are not needed for comparison purposes.

Figure 11 shows a typical force autocorrelation function, minus the equilibrium force squared [see Eq. (66)], for the particle-sphere system. Fluid molecule interactions with the particle and external sphere were taken to be the simple LJ type. Simulation parameters are given in Table 4, and the friction tensor for various separation distances is given in Figs. 12 and 13. As can be seen from Fig. 12, both molecular dynamics and continuum

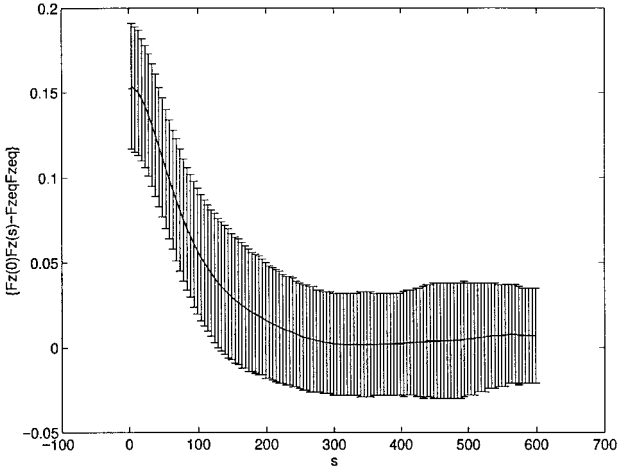

Fig. 11. Typical force autocorrelation function (minus the equilibrium average force squared) for the simple LJ interaction in the particle-sphere system at a separation distance of 1.1d. Note that the force and time shown are dimensionless using the characteristic force as $48\varepsilon/\sigma$ and the characteristic time as $[m\sigma^2/(48\varepsilon)]^{1/2}$.

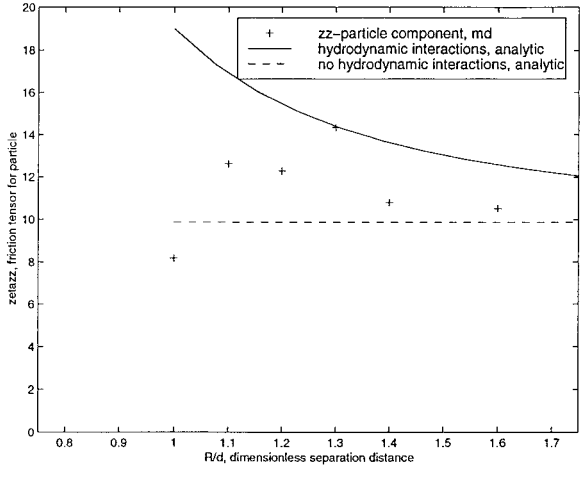

Fig. 12. The particle friction tensor as a function of the separation distance for the simple LJ interaction in the particle-sphere system-component along the line of centers. The particle and the sphere diameter are both 5σ and the friction tensor shown is dimensionless using the characteristic value of $[\sigma^2/(m48\varepsilon)]^{-1/2}$.

hydrodynamic theories predict an increase in the particle friction for surface to surface separation distances greater than two to three molecular diameters. For distances less than this, however, the agreement breaks down due to a break-down in the continuum hypothesis. Similar results in a two-sphere system have been obtained by Vergeles *et al.*[21] using a moving sphere simulation method and Bocquet *et al.*[22] for two Brownian particles.

For the transverse component of the particle friction tensor given in Fig. 13, it can be seen that the MD evaluation of the friction tensor in the particle-sphere system cannot distinguish effects that amount to a 20 to 30% change from the isolated particle results, for the given parameter settings, due to the random errors present. As mentioned before the random errors can only be reduced at the expense of larger systems and larger simulation times. Note that a typical simulation run for the particle-sphere system given above (100,000 time steps) took approximately 24 hr on a SUN workstation ($\sim$30 Megaflop machine). We also note that for the single-particle and particle-sphere systems, the control box length was taken to be two to four times the particle diameter (Tables 2 and 4, respectively). The effects of the finite size of the control volume on the particle friction appeared minimum over this range. However, more extensive studies in larger control volumes are necessary for a more comprehensive experimental analysis.[22]

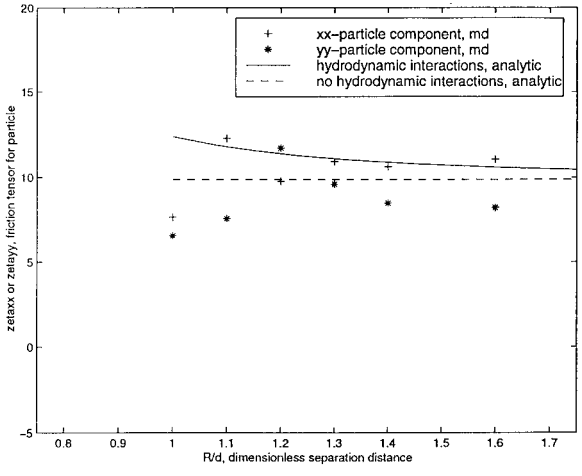

Fig. 13. The particle friction tensor as a function of the separation distance for the simple LJ interaction in the particle-sphere system-components perpendicular to the line of centers. The particle and the sphere diameter are both 5σ and the friction tensor shown is dimensionless using the characteristic value of $[\sigma^2/(m48\varepsilon)]^{-1/2}$.

Table 4. Single Particle near a Fixed External Sphere: Simulation Parameters

Particle diameter/σ, $d/\sigma = 5.0$
External sphere diameter/σ, $b/\sigma = 5.0$
Simple LJ interaction
Effective diameters/$\sigma = 6.0$
Control box length, $l_x/\sigma = l_y/\sigma = 11.0$, $l_z/\sigma = 22.0$
Total number of molecules in control volume = 1766
$T^* = T/(\varepsilon/k) = 1.0017$, $\rho^* = 0.725$
Time step: $\Delta t = 0.5 \times 10^{-14}$ sec.
Total time steps = 100,000

Finally, Fig. 14 shows the equilibrium average fluid force on the particle and the sphere in the particle-sphere system. As expected, the equilibrium force on the particle and sphere is equal and opposite resulting in a net attractive force. Note that these results are consistent with the well-known Asakura–Oosawa potentials popularized in polymer physics.[23]

4. CONCLUSIONS

The Fokker–Planck (FP) equation for a single Brownian particle near a surface has been derived beginning with the Liouville equation written for

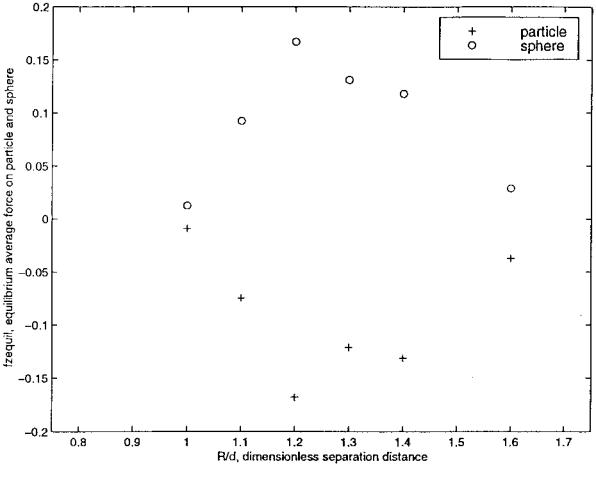

Fig. 14. Molecular dynamics calculation of the equilibrium average force (exerted by the fluid) on the particle and sphere in the particle-sphere system as a function of the Separation distance–component along the line of centers. The particle and the sphere diameter are both 5σ and the force is dimensionless using the characteristic force as $48\varepsilon/\sigma$.

a system consisting of n-fluid molecules, a single rigid particle, and a fixed external surface. The multiple time scales perturbation method was used, which is based on a large mass ratio, $M/m \gg 1$, where M is the mass of the Brownian particle and m is the mass of a fluid molecule. The FP equation includes an explicit expression for the time-independent friction tensor of a single Brownian particle near a surface in terms of the force autocorrelation function (FAF). It was shown that the FAF must decay rapidly on the τ_0 time scale, which physically requires $N_{\mathbf{Kn}} \ll 1$ where $N_{\mathbf{Kn}}$ is the Knudsen number (ratio of the length scale for fluid intermolecular interactions to the characteristic length scale for the Brownian particle). The FAF is to be evaluated under the conditions of equilibrium of the fluid molecules in the presence of a fixed particle and a fixed external surface.

Specific molecular dynamics simulations were carried-out to determine the friction tensor for systems characterized by Lennard–Jones molecular interaction potentials. Predicted friction coefficients for a single spherical particle in the absence of any external surface were shown to agree with Stokes' Law for "stick" boundary conditions provided that effective sphere diameters were used. These results are consistent to those previously given by Alley and Alder[16] for hard sphere systems. Additionally, analytical expressions for the static force correlation function were shown to agree extremely well with molecular dynamic results. Static force correlation analysis can also be used to obtain an approximate expression for the friction coefficient for particles in rarefied gas flows and purely repulsive, gas-particle interactions. The expression is shown to compare favorably to Epstein's classical formula. More importantly, the analysis illustrates a remarkable principle of "force-time parity," i.e., the static force correlation values are directly proportional to the "hardness" of the potential, whereas the decay times of the force autocorrelation are inversely proportional to the hardness. The net result is the friction tensor, which is the time integral of the force autocorrelation function, is independent of the "hardness" index or specific potential type. Molecular dynamics results demonstrate that force-time parity also holds in dense, liquid systems as well, explaining why Stokes' law holds for such a wide range of types of particles and fluids.

Molecular dynamic simulations were also carried-out for a single particle near a spherical external surface (adsorbate). Fluid molecule interactions with the particle and the external surface were taken to be simple LJ as discussed previously. Molecular dynamics results were then compared to continuum hydrodynamic theories. In general, MD simulations showed the increase in the hydrodynamic resistance of a single particle near a surface for large separations qualitatively consistent with hydro-

dynamic theories. However, MD results demonstrated a decrease in the friction tensor as the surface-to-surface separation distance becomes smaller, approaching a distance on the order of a couple of molecular diameters.

Finally, we note that the analysis given here neglects the rotational motion of the Brownian particle and treats only the translational motion. Extensions to rotational motion, including a fixed external surface are currently being developed.[24]

APPENDIX

To see Eq. (56), we first note that

$$e^{-N_{\mathrm{Kn}}^{-1} L_f s}\mathbf{F}_f = \mathbf{F}_f - sN_{\mathrm{Kn}}^{-1} L_f \mathbf{F}_f + \frac{s^2 N_{\mathrm{Kn}}^{-2}}{2} L_f^2 \mathbf{F}_f \cdots \tag{A1}$$

Also, $\mathbf{F}_f$ depends implicitly on time through the fluid molecular phase-space variables $\mathbf{q}$, i.e., by the chain rule

$$\frac{d\mathbf{F}_f(t)}{dt} = N_{\mathrm{Kn}}^{-1} L_f \mathbf{F}_f \tag{A2}$$

and

$$\frac{d^2\mathbf{F}_f(t)}{dt} = N_{\mathrm{Kn}}^{-2} L_f^2 \mathbf{F}_f \tag{A3}$$

etc.

Now, it can be seen that Eq. (57) is simply a Taylor series expansion of $\mathbf{F}_f(-s)$ about $\mathbf{F}_f(0)$, i.e.,

$$\mathbf{F}_f(-s) = \mathbf{F}_f(0) - s\frac{d\mathbf{F}_f(0)}{ds} + \frac{s^2}{2}\frac{d^2\mathbf{F}_f(0)}{ds^2} \cdots \tag{A4}$$

where the time derivatives are related to the space derivatives according to Eqs. (A2), (A3), etc., similarly, $\mathbf{F}_f e^{-N_{\mathrm{Kn}}^{-1} L_f s}\mathbf{F}_f$, appearing in Eq. (54), is a Taylor series time expansion of $\mathbf{F}_f(0)\,\mathbf{F}_f(-s)$ about $\mathbf{F}_f(0)\,\mathbf{F}_f(0)(QED)$.

ACKNOWLEDGMENTS

This study was supported by the National Science Foundation under Grant CTS-9633495.

REFERENCES

1. R. Lamanna, M. Delmelle, and S. Cannistraro, Solvent Stokes–Einstein violation in aqueous protein solutions, *Phys. Rev. E* **49**:5878–5880 (1994).
2. R. Lamanna and S. Cannistraro, Water proton self diffusion and hydrogen bonding in aqueous human albumin solutions, *Chem. Phys. Lett.* **164**:653-656 (1989).
3. M. H. Peters, Nonequilibrium molecular dynamics simulation of free molecule gas flows in complex geometrices with application to Brownian motion of aggregate aerosols, *Phys. Rev. E* **50**:4609–4617 (1994).
4. R. I. Cukier and J. M. Deutch, Microscopic theory of Brownian motion: The multiple-time scale point of view, *Phys. Rev.* **177**:240–244 (1969).
5. G. Nienhuis, On the microscopic theory of Brownian motion with a rotational degree of freedom, *Physica* **49**:26–48 (1970).
6. J. Piasecki, L. Bocquet, and J.-P. Hansen, Multiple time scale derivation of the Fokker–Planck equation for two Brownian spheres suspended in a hard sphere fluid, *Physica A* **218**:125–144 (1997).
7. J. Piasecki, Time scales in the dynamics of the Lorentz electron gas, *Am. J. Phys.* **61**:718–722 (1993).
8. J. T. Hynes, Transient initial condition effects for Brownian particle motion, *J. Chem. Phys.* **59**:3459–3467 (1973). Also see: E. L. Chang and R. M. Mazo, On the Fokker–Planck equation for the linear chain, *Mol. Phys.* **28**:997–1004 (1974).
9. R. M. Mazo, On the theory of Brownian motion. II. Nonuniform systems, *J. Stat. Phys.* **1**:101–106 (1969).
10. T. J. Murphy and J. L. Aguirre, Brownian motion of N interacting particles, *J. Chem. Phys.* **57**:2098 (1972).
11. M. H. Peters, Phase space diffusion equations for single Brownian particle motion near surfaces, *Chem. Eng. Comm.* **108**:165–184 (1991).
12. D. W. Heermann, *Computer Simulation Methods in Theoretical Physics*, 2nd Ed. (Springer-Verlag, New York, 1990). An alternative method to velocity rescaling is the use of Nosé–Hoover Mechanics: S. Nosé, *J. Chem. Phys.* **81**:511 (1984); W. G. Hoover, *Phys. Rev. A* **31**:1695 (1985).
13. M. P. Allen and D. J. Tildesley, *Computer Simulation of Liquids* (Oxford Science Publications, New York, 1989).
14. J. M. Haile, *Molecular Dynamics Simulation* (Wiley, New York, 1992).
15. D. Tabor, *Gases, Liquids and Solids and Other States of Matter*, 3rd Ed. (Cambridge, New York, 1991).
16. W. E. Alley and B. J. Alder, *Phys. Rev. A.* **27**:3158–3173 (1983). B. J. Alder and W. E. Alley, *Physics Today*, January, 56–63, 1984. Also see J. J. Brey and J. G. Ordóñez, *J. Chem. Phys.* **76**:3260–3263 (1982).
17. J. P. Boon and S. Yip, *Molecular Hydrodynamics* (McGraw-Hill, New York, 1980).
18. P. S. Epstein, On the resistance experienced by spheres in their motion through gases, *Phys. Fluids* **1**:710–733 (1923).

19. G. M. Torrie, P. G. Kusalik, and G. N. Patey, Molecular solvent model for an electric double layer, *J. Chem. Phys.* **88**:7826–7840 (1988).
20. D. J. Jeffrey and Y. Onishi, Calculation of the resistance and mobility functions for two unequal rigid spheres, *J. Fluid Mechanics* **139**:261–290 (1984).
21. M. Vergeles, P. Keblinski, J. Koplik, and J. R. Banavar, Stokes drag at the molecular level, *Phys. Rev. Lett.* **75**:232–235 (1995).
22. L. Bocquet, L., J.-P. Hansen, J. Piasecki, Friction tensor for a pair of Brownian particles, *J. Stat. Phys.* **89**:321–347 (1997).
23. S. Asakura and F. Oosawa, Interaction between particles suspended in solutions of macromolecules, *J. Polymer Sci.* **33**:183–192 (1958).
24. M. H. Peters, Combined rotational and translational motions of an arbitrarily-shaped Brownian particle near a surface, *J. Chem. Phys.*, to appear (1999).